ACS Catalysis

RESEARCH ARTICLE

pubs.acs.org/acscatalysis

Cyclohexene Epoxidation with Cyclohexyl Hydroperoxide: A Catalytic Route to Largely Increase Oxygenate Yield from Cyclohexane Oxidation

Bart P. C. Hereijgers,[†] Rudy F. Parton,[‡] and Bert M. Weckhuysen*[,†]

[†]Inorganic Chemistry and Catalysis group, Debye Institute for NanoMaterials Science, Utrecht University, Universiteitsweg 99, 3584 CG Utrecht, The Netherlands

[‡]DSM Research Industrial Chemicals, P.O. Box 18, 6160 MD Geleen, The Netherlands

Supporting Information

ABSTRACT: The industrially important deperoxidation reaction of cyclohexyl hydroperoxide was combined with the epoxidation of cyclohexene over a series of mesoporous titanium silicates. The process was found to proceed with high selectivity, forming cyclohexanol, cyclohexanone, and epoxy-cyclohexane. The deperoxidation and epoxidation reactions were found to compete. However, by changing the surface hydrophobicity of the catalysts or the applied olefin/peroxide ratio, the overall mechanism could be directed in favor of the epoxidation. In this way, the combined selectivity toward valuable alicyclic oxygenates from cyclohexane oxidation based on peroxide conversion could be increased up to 170%. The catalysts where found to be stable from recycling and filtration experiments.

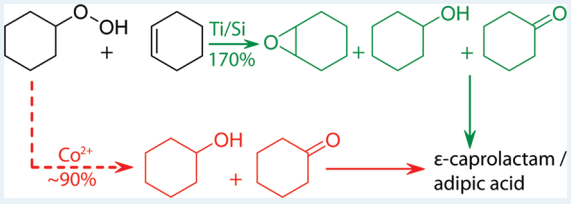

KEYWORDS: selective oxidation, olefin, titanium, TS-1, heterogeneous catalysis

1. INTRODUCTION

The selective oxidation of cyclohexane to a mixture of the corresponding ketone and alcohol (KA-oil) is a key step in the production of nylon-6 and nylon-6,6 polyamides with a production of over 10^6 tons per year.[1,2] In a one-pot approach, cyclohexane is oxidized at 150−170 °C under O_2 pressure, yielding cyclohexyl hydroperoxide (CyOOH) as the first intermediate, which decomposes in the presence of a transition metal salt via a complex radical-chain reaction into both the desired ketone and alcohol. Because of the occurrence of a radical-chain mechanism, byproduct formation is excessive and commercially the process is kept at 4% conversion, achieving a KA-oil selectivity (S_{KA}) of 70−85%.[2−5] In an alternative two-step process, commercially applied by DSM (Oxanon), cyclohexane is oxidized with O_2 into an oxidate mixture containing mainly CyOOH (0.1−8 wt %), and smaller amounts of the decomposition products and acids.[6] Catalytic decomposition of CyOOH over a homogeneous cobalt salt in a subsequent reaction yields KA-oil with a higher overall selectivity. The main drawback of the latter approach is the consumption of large amounts of alkaline solutions in the decomposition step to neutralize the formed carboxylic acids.[6] Although extensive research on the development of efficient and stable heterogeneous and biomimetic catalyst systems has been conducted during the past decades, no breakthrough leading to novel applied catalyst systems has been achieved.[1,5,7−10]

In the current paper, we present a novel catalytic process to largely increase the alicyclic oxygenate yield of CyOOH decomposition by combining the deperoxidation reaction with the epoxidation of cyclohexene (Cy=H) to form a mixture of KA-oil and 1,2-epoxycyclohexene (CyO) over titanium-silica based catalyst materials, as illustrated in Scheme 1. The formed CyO can be distilled off as a valuable industrial intermediate for fine-chemicals production,[11−14] but can as well be converted by hydrogenolysis into cyclohexanol (CyOH),[15] or isomerized to cyclohexanone (Cy=O)[16,17] for downstream processing into adipic acid or ε-caprolactam, respectively.[18] The remainder cyclohexene can be hydrogenated into cyclohexane and recycled into the oxidation stage, thus avoiding a complicated cyclohexane/cyclohexene separation step. The presented process has implications for the production of a wide variety of epoxides from other olefins as well.[19]

2. EXPERIMENTAL SECTION

2.1. Catalyst Materials. SBA-15 was prepared by the procedure as described by Zhao et al.,[20] and MCM-41 was synthesized according to the method by Cheng et al.[21] Titanium grafted SBA-15 materials (in sample code: Ti-G#-SBA, # = Si/Ti) were prepared in a glovebox under N_2 atmosphere. An amount of titanium-isopropoxide (Ti-$^i(OC_3H_7)_4$ Sigma Aldrich 99%) to achieve the desired Si/Ti ratio (Si/Ti = 20, 40, 80, and 120) was dissolved in anhydrous isopropanol and impregnated on SBA-15 using the wetness impregnation method (3.3 mL ^{i}propanol per g of SBA-15 was applied). The solvent was removed by drying

Received: July 4, 2011
Revised: July 12, 2011
Published: August 15, 2011

Scheme 1. Novel Catalytic Tandem Process and the Commercially Applied Route of CyOOH Deperoxidation

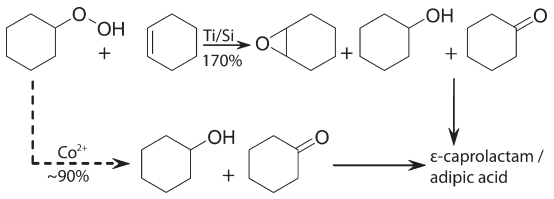

under N_2 flow at room temperature for 48 h followed by calcination at 400 °C for 4 h.[22,23] As reference materials TiO_2 P25 (Degussa), TS-1, and Ti-BEA were used. For the experiments using Co^{2+}, cobalt-methylhexanoate (Sigma Aldrich, 65 wt % in mineral spirits) was used.

2.2. Catalyst Characterization. Diffuse Reflectance (DR) UV−vis spectra were recorded on a Varian Cary 500 spectrophotometer in the range of 200−800 nm using a Halon white standard as reference material. Thermogravimetric analysis (TGA) was performed on a TA Instruments Q50 apparatus in a N_2 flow. N_2-physisorption measurements were done on a Micromeretics Tristar 3000 analyzer. Prior to analysis the samples were dried at 250 °C for at least 12 h. Small Angle X-ray Diffraction (XRD, 2θ = 0.7−5°) was performed on a Bruker AXS D2 Phaser apparatus using a $Co_{K\alpha}$ radiation source (λ = 1.78897 Å) operating at 30 kV and 10 mV.

2.3. Catalytic Performance. Batch catalytic tests were performed in a 100 mL round-bottom flask equipped with a reflux condenser and septum. Fifteen grams of a 2 wt % cyclohexyl hydroperoxide (2.6 mmol CyOOH) solution in cyclohexane (Sigma Aldrich, 99%) containing 1 mol % biphenyl and the amount of cyclohexene (Sigma Aldrich, 99%) for the desired olefin/peroxide (O/P) ratio were loaded into the reactor together with 50 mg of catalyst and placed in an oil bath at 80 °C. Aliquots were taken from the reactor with a syringe through a septum during reaction and quenched in pyridine (Sigma Aldrich, 99%) precooled at −20 °C. Prior to analysis, liquid samples were silylated with *N*-methyl-*N*-trimethylsilyl-trifluoro-acetamide (MSTFA, ABCR, 98%). The silylated samples were analyzed by GC-FID using a Varian 430 GC, equipped with a VF-5 ms column (30 m, DF = 0.25 μm, I.D. = 0.25 mm) in split/splitless injection mode. The injector temperature was set to 220 °C.[8]

2.4. Cyclohexyl Hydroperoxide Extraction. The cyclohexyl hydroperoxide was extracted from cyclohexane oxidate provided by DSM. First 250 mL of oxidate was extracted 3 times with 50 mL of 1 M NaOH (Merck, p.a.). The water phase was neutralized with cooled 4 M HCl (Merck, p.a.) until slightly acidic. Then, the water phase was extracted 3 times with ∼30 mL of cyclohexane and dried over $MgSO_4$ (Janssen Chimica, pure). Eventually ∼1 mol % biphenyl (Acros. 99%) was added to determine the CyOOH concentration by GC, followed by dilution with cyclohexane to obtain a 2 wt % solution of CyOOH. The starting reaction mixture typically contained some impurities, that is, 0.2 mol % CyOH, 0.1−0.2 mol % Cy=O, 0.01 mol % butyric acid, 0.08 mol % valeric acid, and 0.08 mol % caproic acid coming from the oxidate and 0.03 mol % cyclohexenyl hydroperoxide from cyclohexene.

3. RESULTS AND DISCUSSION

3.1. Catalyst Characterization. There is general consensus in the literature that isolated tetrahedral Ti^{4+} species are involved in the epoxidation of for instance propylene with hydrogen peroxide over titanium-silicalite catalyst materials. One of the possible functions the isolated titanium centers have is the formation of titanium hydroperoxo species (Ti-OOH) which are, one way or another, involved in the epoxidation process.[24−26] Diffuse Reflectance (DR) UV−vis spectroscopy provides a sensitive tool for the characterization of the coordination environment of Ti^{4+} species.[22,27−30] Figure 1 shows the UV−vis DR spectra of the fresh Ti−Si catalyst materials. Plain SBA-15 is included as a titanium free reference compound, TiO_2 P25 as the bulk reference compound with Ti^{4+} octahedrally coordinated and Ti-BEA as a tetrahedral Ti^{4+} reference compound. An absorption band at 210 nm is clearly visible for the Ti-BEA material, which is characteristic for the presence of isolated Ti^{4+} species in tetrahedral coordination, exhibiting a strong absorption band in the UV-region because of the ligand-to-metal charge transfer (LMCT) of oxygen to a titanium center.[22,23,31,32] For the titanium grafted SBA-15 materials this absorption band is slightly shifted to 220 nm, indicating a distorted tetrahedral geometry, a direct consequence of the amorphous walls of SBA-15.[23,29,30,33] The UV−vis DR spectra of Ti-G80-SBA and Ti-G120-SBA overlapped completely.

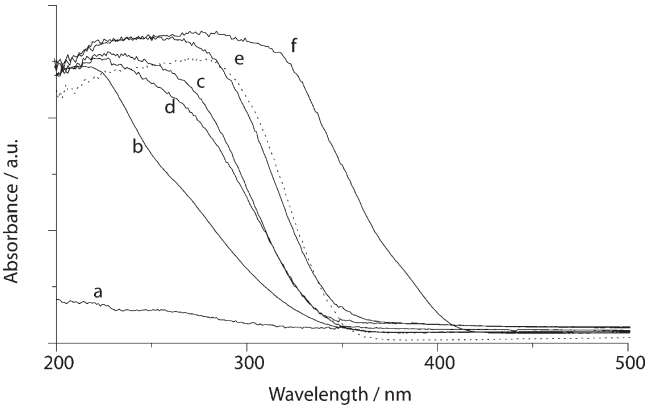

Figure 1. UV−vis DR spectra of fresh Ti-SiO_2 materials: SBA-15 (a), Ti-BEA (b), Ti-G120-SBA and Ti-G80-SBA (c), Ti-G40-SBA (d), Ti-G20-SBA (e), TiO_2 P25 (f) and Ti-G120-SiO_2 (dotted line).

Next to this absorption band a shoulder with a maximum around 250 nm is visible. This absorption band can be ascribed to Ti species in 5-fold and 6-fold coordination because of the coordination of one or two water molecules,[23,29,30] but is also ascribed to the occurrence of Ti−O−Ti oligomers.[28] However, the position of the absorption edge at 330 nm corresponds to the position found for Ti-BEA and no shift in the edge energy is observed when increasing the Ti loading in the Si/Ti range of 120−40. This indicates that in this range, the coordination is independent of the loading and therefore it is concluded that at least the majority of the Ti population is present as isolated species. For the Ti-G20-SBA and Ti-G120-SiO_2 materials the LMCT band became broader and red-shifted to 280−290 nm. Additionally, the edge energy shifted to 360 nm, indicating that the Ti^{4+} sites are no longer completely isolated, but exist as Ti−O−Ti oligomers.[28,34] The broad absorption band between 350−400 nm, as is observed for TiO_2 P25, is absent for all samples indicating the absence of extra framework TiO_2 in the Ti/Si materials.[27,31,34] This is in agreement with results published by Gao et al., who only found the formation of anatase at loadings exceeding 15 wt % TiO_2 on a SiO_2 aerogel.[22]

dx.doi.org/10.1021/cs200354c |*ACS Catal.* 2011, 1, 1183–1192

Table 1. TGA Results of Different SBA-15 and MCM-41 Based Ti-Grafted Materials[a]

catalyst	weight loss 1 (%)	weight loss 2 (%)
SBA-15	10.2	1.4
MCM-41	0.85	1.2
Ti-G40-SBA	10.4	0.2
Ti-G80-SBA	9.5	0.3
Ti-G80-MCM	7.8	1.1
SBAp900	0	0
Ti-G80-SBAp900	1.0	0

[a] Weight loss 1 represents the first heating stage to 150°C, while weight loss 2 represents the second heating stage to 500°C.

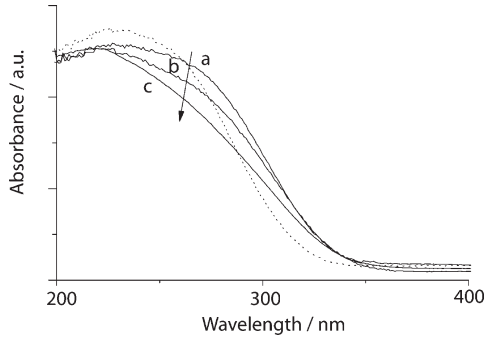

Figure 2. UV−vis DR spectra of Ti-G80-SBA (a), Ti-G40-SBA (b), Ti-G80-SBAp900 (c), and Ti-G80-MCM (dotted line).

Upon calcination of the support material at 900 °C prior to (SBAp900) and after (SBAc900) Ti-grafting, surface hydroxyl groups are removed from the SBA-15 surface. This leads to a more hydrophobic character of the support material as was verified by TGA,[35] the results of which are summarized in Table 1.

When heating the sample to 150 °C, the physisorbed water desorbs from the sample, resulting in a weight loss of 10.4 wt % for as-synthesized SBA-15. In the second heating stage to 500 °C, also the surface hydroxyls will desorb as water vapor.[35,36] For the bare SBA-15 material this resulted in a weight loss of 1.4 wt %. After grafting Ti onto the surface of SBA-15 the amount of physisorbed water seems merely unaffected as evidenced from the weigth loss at 150 °C for the Ti-G40-SBA and Ti-G80-SBA materials of 10.4 and 9.5 wt %, respectively. However, the amount of surface hydroxyls has significantly decreased because of reaction of the titanium atoms with the surface hydroxyl groups.[22] When comparing the UV−vis DR spectrum of Ti-G40-SBA to Ti-G80-SBA in Figure 2, a decrease in intensity of the absorption band at 250 nm is observed. Since the higher Ti loaded sample is expected to have a higher number of Ti−O−Ti oligomers and thus an increased absorption in the higher wavelength region as compared to the lower loaded Ti-G80-SBA material,[22,30] this indicates that the absorption band is indeed caused by sample hydration rather than the presence of Ti−O−Ti bonds.

From the TGA results it is evident that after calcining SBA-15 at 900 °C and equilibration in air, almost no physisorbed water is anymore present in the sample. Moreover, also the surface hydroxyl groups are removed, which results in a more hydrophobic support material. After Ti-grafting, this still holds, as only 1.0 wt % water is released from the sample below 150 °C and no significant change in sample weight was observed when heating to 500 °C. The decrease in physisorbed water is also reflected in the corresponding UV−vis DR spectrum (Figure 2) as the shoulder at around 260 nm has largely decreased in intensity for the Ti-G80-SBAp900 sample. Following the same reasoning, from TGA weight loss and the UV−vis DR spectra, it can be concluded that the Ti-G80-MCM-41 support is more hydrophobic when compared to SBA-15.

Table 2. N_2-Physisorption Data of the SBA-15, Ti-G40-SBA, and SBAp900 Materials and Surface OH Group Density As Derived from N_2-Physisorption and TGA[35]

material	BET surface area (m^2/g)	total pore volume (cm^3/g)	pore diameter (nm)	OH-group density (nm^{-2})
MCM-41	1002	0.97	4.0	0.69
SBA-15	879	1.00	6.1	1.01
Ti-G40-SBA	535	0.64	5.9	0.46
SBAp900	270	0.34	4.9	<0.05[a]
Ti-SBAp900	308	0.37	4.8	<0.05[a]
Davicat SI1351[b]	328	1.2	14	2.7
Davicat SI1404[b]	458	0.87	7.6	2.9

[a] based on a weighing precision of 0.01% for the TGA instrument. [b] The Davicat silica gels are included as hydrophilic reference compounds.

By relating the N_2-physisorption data to the TGA results, surface OH group densities can be obtained for the different materials, as listed in Table 2. It is confirmed that indeed the amount of surface OH-groups decreased significantly upon Ti grafting from 1 nm^{-2} to 0.46 nm^{-2}. Upon high temperature treatment the surface OH-group density decreased to virtually zero. The obtained numbers are in good agreement with results published earlier.[35] The OH-group density of the SBAp900 sample did not change after Ti-grafting and storage in air, indicating that the silanol bridges formed during high temperature treatment are stable against rehydration by moisture and isopropanol. Comparison with the surface OH-group density of the commercial high surface area silica gels by Davicat of 2.7 nm^{-2} and 2.9 nm^{-2} illustrates the relative hydrophobic nature of the catalytic materials.

The change in surface area of the materials after Ti-grafting and high temperature treatment has been verified by N_2-physisorption. The isotherms and pore size distributions of some relevant materials are presented in Figure 3, panels I and II. Numerical results are listed in Table 2. Comparison of the isotherms of SBA-15 (a) and Ti-G40-SBA (b) indicates that upon Ti-grafting some surface area and pore volume is lost. This is reflected by a decrease of the Brunauer−Emmett−Teller (BET) surface area from 880 to 535 m^2/g. However, the porous structure remains largely intact as can be concluded from the shape of the hysteresis loop, the position of the capillary condensation, and the sharp pore size distribution. This indicates that no TiO_2 particles are formed, as those would affect the pore shape and diameter significantly and thus change the shape and position of the hysteresis. The loss in surface area after Ti grafting can be explained by the SBA-15 pore corrugation[37] and pore wall porosity. By grafting, the titanium ions attach to the silanol groups on the pore surface.[22] Most likely they anchor in between the ridges of the SBA-15 mesopores and within the microporous walls, to obtain a tetrahedral coordination more easily. In this way, the rugged surface of the pore is flattened and micropores are filled resulting in a loss of surface area, while leaving the

dx.doi.org/10.1021/cs200354c |ACS Catal. 2011, 1, 1183–1192

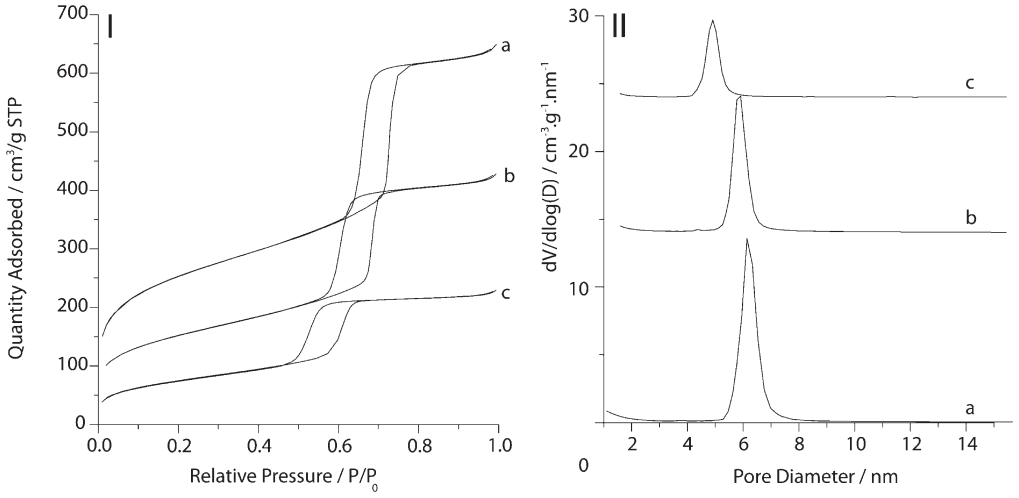

Figure 3. N_2-physisorption isotherms (I) and pore size distribution (II) of the SBA-15 (a), Ti-G40-SBA (b), and SBAp900 (c) materials.

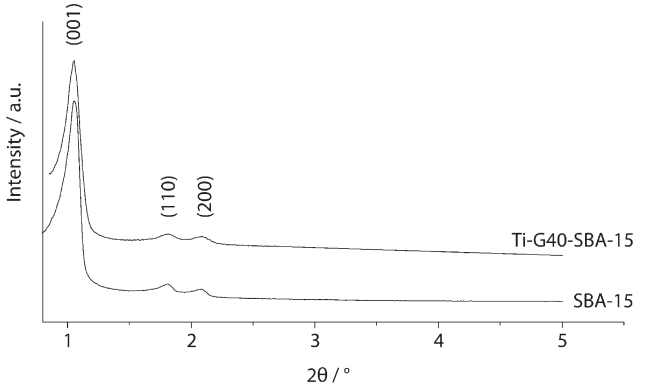

Figure 4. Powder XRD patterns of the calcined SBA-15 and Ti-G40-SBA materials.

average mesopore diameter virtually unaffected. In the case of SBAp900, the BET surface area and pore volume have largely decreased as well, although again the SBA-15 structure is preserved as indicated by the hysteresis loop and the sharp pore size distribution. The structural shrinkage and consequent decrease of surface area and pore diameter of SBA-15 after high temperature treatment were also observed by Shin et al.[38]

Preservation of the SBA-15 structure after Ti-grafting on the SBA-15 support was also confirmed by X-ray diffrcation (XRD). The XRD patterns of SBA-15 and Ti-G40-SBA are shown in Figure 4. In both patterns, the (001), (110), and (200) Bragg reflections are present at 2θ values 1.05°, 1.81°, and 2.09° confirming the hexagonal symmetry (*P6mm*) of the pores.[20,39]

3.2. Catalytic Performance. The conversion and selectivity of a cyclohexene epoxidation reaction versus time on stream for the Ti-G40-SBA (I) and Ti-G80-SBA (II) catalyst materials are presented in Figure 5. It seemed that the CyOOH conversion leveled off with time on stream, which is in line with the quasi first order kinetics in CyOOH concentration as reported before for different catalyst systems.[40,41]

The selectivity toward CyOH and CyO, the expected products of the epoxidation reaction, was high immediately from the start of the reaction and reached 84% and 67%, and 69% and 54% for Ti-G40-SBA and Ti-G80-SBA, respectively. In both cases the production of Cy=O was low, but increased with time on stream. For the more selective Ti-G40-SBA catalyst, the Cy=O formation is significantly lower as compared to Ti-G80-SBA. Other reactions that might occur under these conditions are the allylic oxidation, yielding cyclohexenol and cyclohexenone and the hydrolysis of the epoxide into 1,2-cyclohexyldiol. Of those, only cyclohex-2-ene-1-one and cyclohexenyl hydroperoxide were observed in small, but significant quantities (2−7% selectivity at 24 h on stream). The formation of organic acids was negligible and within the experimental error (± 2%) as shown in Figure 6. In Table 3, the results as obtained for different SBA-based Ti-silicates and benchmark materials TiO_2 P25, Ti-BEA, and Co^{2+} after 24 h reaction are summarized. The archetype TS-1 epoxidation catalyst was employed as well, reaching only 5.5% conversion after 24 h reaction. This low activity is ascribed to the pore size of the MFI topology (5.5 × 5.1 Å), which is of similar dimensions as the kinetic diameter of the peroxide and the solvent (5.8 Å for cyclohexane).[42] We employed our Ti-grafted SBA-15 catalyst materials for epoxidation with aqueous H_2O_2 and TBHP as well. However, the apolar cyclooctane medium prevented an adequate mixing between the catalyst, olefin, and hydroperoxide. Therefore, only a very low activity was observed, and the main product was cyclooctyl hydroperoxide, originating from solvent oxidation (see Supporting Information, Figure S1).

3.3. Influence of the Support Hydrophobicity. In section 3.1, we described the influence of the calcination temperature and Ti/Si ratio on the support hydrophobicity, as was determined from the water and surface hydroxyl group content of the treated SBA-15 materials by TGA. Obviously, in a reaction where polar (CyOOH) and nonpolar (Cy=H) reactants react in an apolar medium (CyH) producing polar products, hydrophilic/hydrophobic properties of the catalyst surface are of major importance. Those characteristics determine the interaction of different species with the active sites, but also can alter the concentration ratios of the different species at the active sites as compared to the bulk.

In Figure 7 (I), the CyOOH conversion and combined selectivity toward CyOH, Cy=O, and CyO versus time is shown. It is clear that the more hydrophobic SBA-15 supports establish a higher initial conversion rate, although the final conversion after 24 h is comparable for all catalysts. The Ti-G80-MCM catalyst reaches the highest initial conversion rate, which cannot solely be explained in terms of surface hydrophobicity. Indeed the TGA

dx.doi.org/10.1021/cs200354c |*ACS Catal.* 2011, 1, 1183–1192

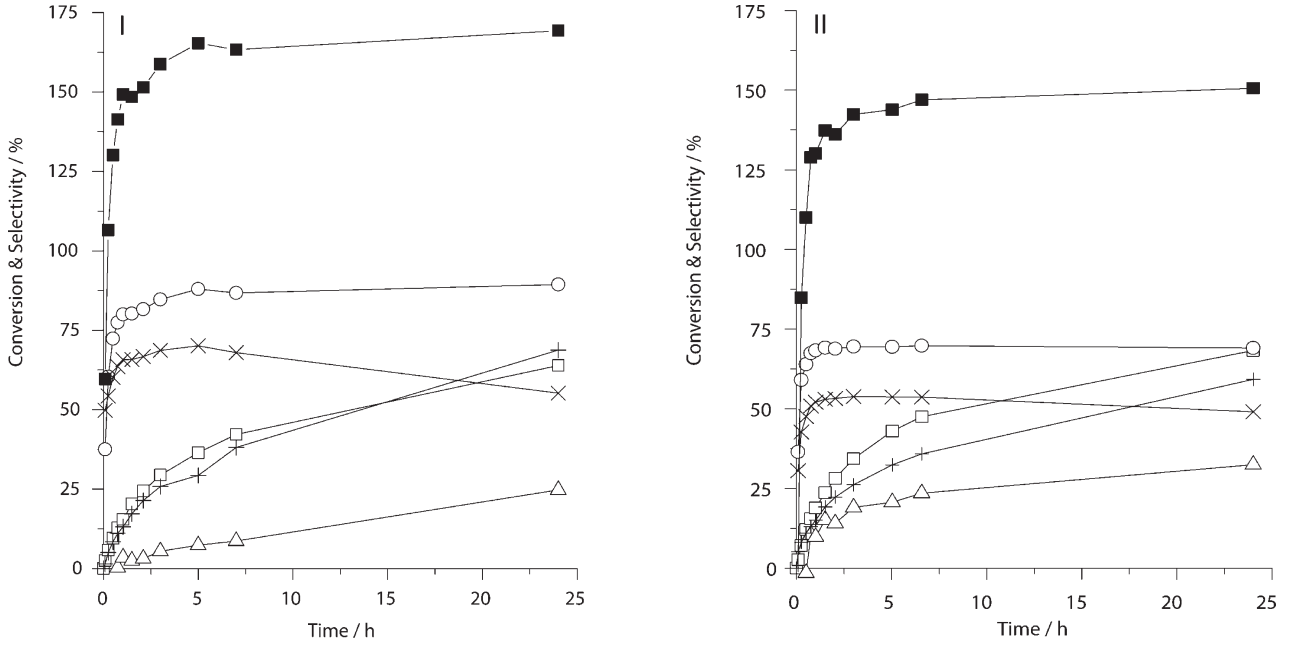

Figure 5. Catalytic performance of Ti-G40-SBA (I) and Ti-G80-SBA (II) in Cy=H epoxidation with CyOOH at 80 °C and an O/P ratio of 1.1. Conversions of CyOOH (□) and Cy=H (+) and product selectivities toward CyOH (○), Cy=O (Δ), and CyO (×) and their sum (■).

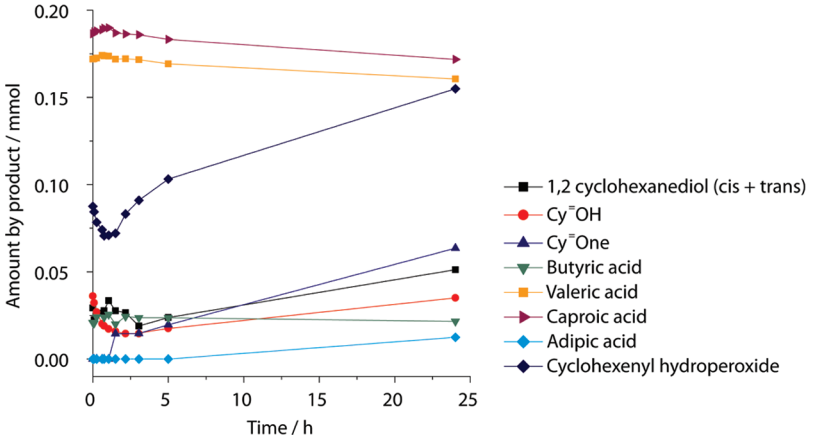

Figure 6. Formation of byproduct in the cyclohexene epoxidation with CyOOH over Ti-G80-SBAp900 at 80 °C.

results indicate that the MCM-41 support is less hydrophobic compared to the SBAp900. Also a significantly higher selectivity is obtained over the more hydrophobic catalysts. The total selectivity to alicyclic oxygenates at 5 h on stream was increased from 127% to 157% when using a SBA-15 catalyst support calcined at 900 °C. For all catalysts except Ti-G80-SBA the selectivity up to 5 h on stream is similar, after which some deviations appear. The highest selectivity after 24 h of 165% is obtained with a Ti-G80-SBAc900 catalyst.

3.4. Influence of the O/P Ratio. To optimize the reaction conditions we have evaluated the influence of the applied bulk Cy=H/CyOOH, or O/P ratio. On the basis of reaction stoichiometry, a ratio of 1 would be expected to be ideal only under ideal circumstances when solely epoxidation takes place. When also a deperoxidation reaction is taking place, a different ratio might be beneficial.

From the results for Ti-G80-SBAp900 as presented in Figure 7 (II), it is observed that when increasing the O/P ratio from 0.9 to 1.1, no significant change in selectivity is observed. However, when increasing the O/P ratio to 1.4, the total selectivity is boosted up to 170% at 24 h on stream. This coincided with a significant decrease in Cy=O selectivity from 45 to 19%. Remarkably, the O/P ratio does not have an effect on the CyOOH conversion rate. Similar results where obtained for the more hydrophilic Ti-G80-SBA. In the case of Ti-G40-SBA, increasing the O/P ration from 1.1 to 1.2 to 1.4 had an adverse effect on the selectivity decreasing from 164 to 144% (Supporting Information, Figure S2).

3.5. Catalyst Stability. Especially in liquid phase reactions, heterogeneous catalysts can be susceptible to deactivation by severe leaching of the active species. For instance, in cyclohexane oxidation many proposed heterogeneous catalyst systems were found not to be truly heterogeneous. A small amount of dissolved transition metal ions can cause significant activity in hydroperoxide decomposition.[6] We have shown before that 1.5 ppm

dx.doi.org/10.1021/cs200354c |ACS Catal. 2011, 1, 1183–1192

dissolved Co^{2+} and even leached ions from a stainless steel vessel wall, exhibit high activity in cyclohexane oxidation.[8]

From the UV−vis DR spectra of a fresh catalyst compared to a spent catalyst as presented in Figure 8, it is clear that the absorption band at 220 nm, corresponding to the isolated Ti-sites, did not decrease after reaction. The absorption band at 250 nm, however, increased significantly, indicating that a larger part of the Ti-sites now is in octahedral sites, possibly because of water coordination. The band at 358 nm has been ascribed to the presence of Ti-OOH species before.[32,43] Nonetheless, it appears that the grafted Ti-species were not subject to severe leaching or sintering. However, it was stated by Sheldon et al. that true heterogeneity can only be proven by separating the catalyst from the reaction mixture.[44] In the case of a true heterogeneous catalyst, the reaction should proceed significantly slower after removal of the catalyst. To prevent re-adsorption of leached active metal ions on the catalyst upon cooling the reaction mixture, "hot-filtration" should be applied. Figure 9 shows the results of an experiment with Ti-G40-SBA. After 90 min reaction, the reaction mixture was filtered hot through a preheated filter, collected in an ice-cooled flask to prevent excessive evaporation and immediately placed back in the oil bath for further reaction.

Table 3. Catalytic Performance of Different Ti/Si Catalyst Materials in the Epoxidation of Cyclohexene with CyOOH at 80°C[a]

catalyst	C_{CyOOH}	$C_{Cy=H}$	CyOH	Cy=O	CyO
Co^{2+}	61	46	88	46	5.5
Ti-BEA	41	49	82	31	42
TiO_2 P25	33	54	60	32	14
Ti-G120-SBA	68	60	68	39	48
Ti-G80-SBA	68	59	69	32	49
Ti-G40-SBA	61	67	87	19	57
Ti-G20-SBA	59	57	74	31	39
Ti-G120-SiO_2	51	58	87	24	58

[a] Conversion and selectivities after 24 h reaction are listed. The applied CyOOH: Cy=H ratio was 1.1. Reported selectivities are based on CyOOH conversion only.

After removing the catalyst, the CyOOH conversion rate constant decreased 1 order of magnitude from $k_{CyOOH} = 4.4 \times 10^{-5}\ s^{-1}$ in the presence of a catalyst to $k_{CyOOH} = 5.0 \times 10^{-6}\ s^{-1}$ after separating the catalyst from the reaction mixture. Moreover, no significant epoxidation activity was observed after removal of the catalyst. On the other hand, the decomposition rate was larger than the value for a pure thermal decomposition in the absence of a catalyst and cyclohexene, which was determined at $k_{CyOOH} = 1.2 \times 10^{-6}\ s^{-1}$. This suggests that after separating the catalyst from the mixture some leached Ti-species, or finely dispersed catalyst particles, that can decompose the hydroperoxide remained. Then again, after removal of the catalyst a steep increase in the allylic oxidation rate was observed. The decomposition of the less stable cyclohexenyl hydroperoxide and radical attack on the olefin contribute to a higher free radical concentration that will accelerate the CyOOH decomposition. Nevertheless, although true heterogeneity of the Ti-sites is not undoubtedly proven, the experimental results clearly show that any possible leaching of Ti is only a minor concern. The slope of Cy=O formation is merely unaffected by the removal of the catalyst, providing additional proof that Cy=O solely originates from CyOOH decomposition and subsequent propagation reactions.

Finally, we evaluated the catalyst stability by two sets of recycling experiments, the results of which are presented in Figure 10. During the first set of recycling experiments the catalyst was

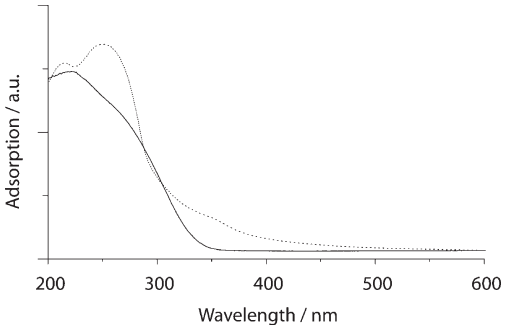

Figure 8. UV−vis DR spectra of fresh (solid line) and spent (dotted line) Ti-G80-SBA before and after an epoxidation reaction for 24 h at 80 °C.

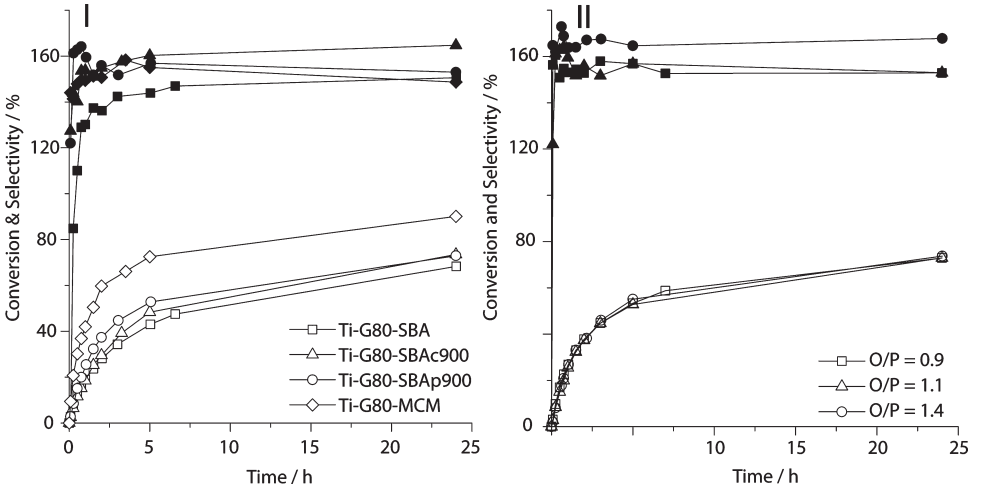

Figure 7. Influence of (I) the catalyst surface hydrophobicity at O/P = 1.1 and (II) the applied O/P ratio over Ti-G80-SBAp900 on the conversion (open symbols) and total selectivity (solid symbols).

dx.doi.org/10.1021/cs200354c |ACS Catal. 2011, 1, 1183–1192

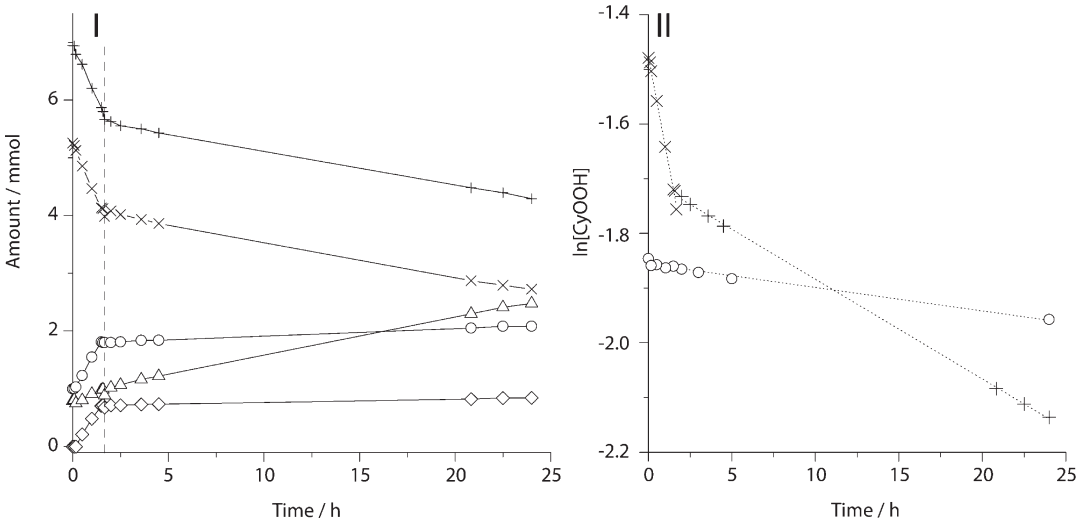

Figure 9. Hot filtration experiment during cyclohexene epoxidation with CyOOH over Ti-G40-SBA at 80 °C. (I) Content of the reaction mixture; CyOOH (×), Cy=H (+), CyOH (○), CyO (◇), and Cy=O (Δ) and (II) integrated first order rate laws before (×, $R^2 = 0.997$) and after (+, $R^2 = 0.997$) separating the catalyst at 90 min on stream and for the thermal CyOOH decomposition (○, $R^2 = 0.979$).

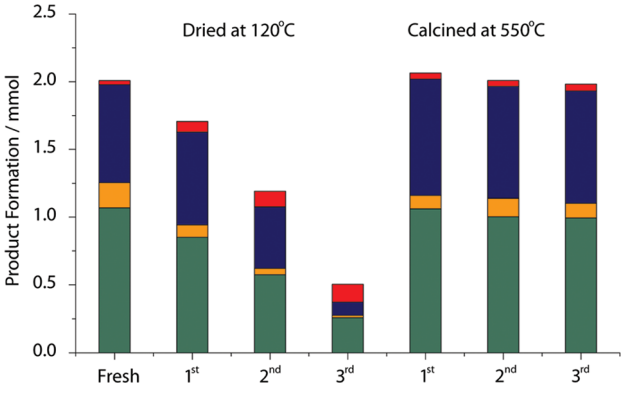

Figure 10. Catalyst recycling experiments. Formation of CyOH (green), Cy=O (orange), CyO (blue), and Cy=OOH (red) in mmol after 5 h reaction at 80 °C over Ti-G40-SBA. From left to right, fresh catalyst and 3 recycling runs after drying at 120 °C after every run, and 3 recycling runs after calcination at 550 °C in between every run.

separated from the reaction mixture after 5 h, washed with acetone, and dried overnight at 120 °C in between every run. It was observed that the product formation after 5 h reaction decreased steeply already in the second run and did not stabilize in subsequent runs. Thus evidently, in this case the catalyst deactivated severely. In a second set of identical recycling experiments, the catalyst was calcined at 550 °C in between every run. It was observed that in this case the product formation after 5 h reaction remained virtually constant. Therefore, we conclude that the catalyst materials indeed deactivate, but not through leaching of the active species, but by deposition of carbonaceous compounds on the catalyst. By calcining the catalyst, the activity could be regenerated completely.

4. DISCUSSION

When comparing the catalytic performance of all different catalyst materials and references from Table 3, it is clear that the reference materials, TiO_2, Ti-BEA, and Co^{2+} display inferior performance as compared to the Ti-grafted materials. For TiO_2 this is due to the lack of isolated Ti^{4+} sites, although being a good photocatalyst, the conversion is much higher than when performing the reaction in the absence of light (5% CyOOH conversion was reached after 24 h in the latter case). Also the activity of Ti-BEA is low, which is most likely a direct effect of the slow diffusion of the peroxide inside the micropores. Besides that, the hydrophilic character of the zeolite and the consequent presence of water coordinating to the Ti^{4+} sites, as indicated by the shoulder at 260 nm in the UV−vis DR absorption spectrum (Figure 1), will impede the reaction. The reference experiment with Co^{2+}, which is commercially employed for CyOOH decomposition via a radical pathway,[5,6,45,46] shows that free radicals are not able to perform the epoxidation with high efficiency. The influence of the Si/Ti ratio of the grafted materials is not obvious in that sense that activity and selectivity do not follow the Si/Ti ratio trend. However, from the reduced activity of the higher loaded Ti-G20-SBA and Ti-G120-SiO_2 that display the formation of TiO_2 nanoparticles, it is clear that isolated Ti^{4+} sites are needed to perform the reaction.

When studying the catalytic data as listed in Table 3 more carefully, some aspects of the reaction deserve more attention here. It is clear that in all cases except for TiO_2, the selectivity toward KA-oil, S_{KA}, reaches more than 100% after 24 h on stream, although both the ketone and the alcohol form directly from CyOOH. The only explanation can be that the fraction of the CyOOH that undergoes a thermally or catalytically driven deperoxidation reaction creates reactive free radicals, which can initiate a radical chain on the ubiquitous cyclohexane molecules as was explained by Hermans et al.[47] This explanation is confirmed by the fact that Co^{2+}, which only causes radical decomposition of the peroxide,[5,7] exhibits the highest S_{KA} of 134%. Under the applied conditions using a Ti−Si catalyst, this reaction is slow and occurs in the time scale of hours and only plays a significant role after 24 h on stream. The occurrence of radical propagation reactions yields new peroxide molecules. This implies that in fact the CyOOH conversion is higher than the numbers reported in Table 3 and explains the observed leveling off of the conversion. In fact, performing a typical epoxidation

dx.doi.org/10.1021/cs200354c |ACS Catal. 2011, 1, 1183–1192

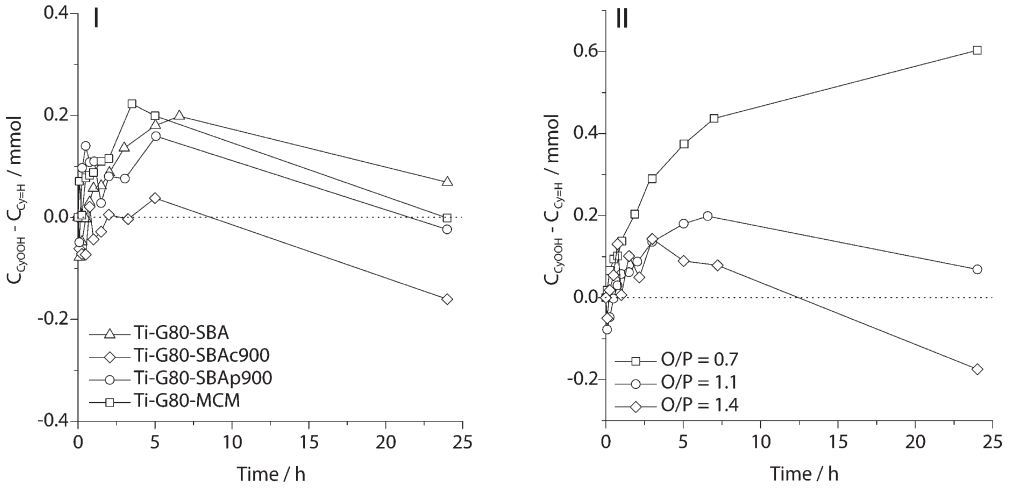

Figure 11. CyOOH conversion minus Cy=H conversion in mmol over (I) different Ti−Si catalyst materials with O/P ratio 1.1 and (II) over Ti-G80-SBA with varying the O/P ratio.

reaction under N_2 atmosphere yielded a CyOOH conversion of 98% after 14 h.

From Figure 11, panels I and II, it can be seen that either changing the support to a more hydrophobic surface or applying a higher O/P ratio has a similar effect on the molar conversion of CyOOH as compared to Cy=H. In all cases, a near equimolar conversion of CyOOH and Cy=H ($C_{CyOOH} - C_{Cy=H} \approx 0$) coincided with a higher overall selectivity toward CyOH + Cy=O + CyO and a lower Cy=O formation rate. This implies that two different reactions involving CyOOH are competing, that is, epoxidation (eq 1) and deperoxidation (eq 2). When heating the hydroperoxide in the absence of cyclohexene in the presence and absence of a catalyst we found 95% and 11% conversion after 24 h, respectively. Thus, indeed the Ti−Si catalysts displayed activity for the deperoxidation reaction, which is most probably acid catalyzed.[48]

$$\text{CyOOH} + \text{Cy=H} \rightarrow \text{CyOH} + \text{CyO} \quad (1)$$

$$(x + y)\text{CyOOH} \rightarrow x\text{CyOH} + y\text{Cy=O} \quad (2)$$

By altering the reaction conditions, either through the catalyst surface hydrophobicity or the O/P ratio, such that there is a relatively high O/P ratio at the reaction site, one can force the reaction to follow the epoxidation pathway, yielding a higher total selectivity. When eq 1 dominates the overall reaction mechanism, an approximate equimolar conversion of CyOOH and Cy=H must be established as is the case under optimum conditions. The contribution of thermal CyOOH decomposition is limited under the applied conditions. Another possible benefit of a more hydrophobic catalyst arises from research by Figueras et al. who found that a more hydrophobic catalyst surface could prevent the hydrolysis of the epoxide ring and the *tert*-butyl hydroperoxide.[49] Although we did not observe significant formation of 1,2-cyclohexanediol, when processing wet commercial cyclohexane oxidate as CyOOH source, suppressing hydrolysis will be a major advantage.

From Figure 11 it is also observed that with increasing time on stream, the molar cyclohexene conversion becomes higher than the CyOOH conversion which, indicates slow evaporation of Cy=H from the reactor. Hence, an incomplete carbon balance is obtained, which makes it impossible to calculate a reliable selectivity of epoxide formation in terms of Cy=H conversion. However, in all cases this selectivity lay between 60 and 80% after 5 h on stream, when the effect of evaporation is clearly less apparent than after 24 h on stream. The oxygenated molecules have a much higher boiling point, so their evaporation loss is less pronounced and an oxygen balance is therefore more reliable. When assuming the formation of equimolar amounts of water and cyclohexanone, which directly follows from the CyOOH decomposition mechanism as reported by Hermans et al.,[47] an oxygen balance over time varying between 94 and 100% is obtained in all cases. Besides that, when calculating the oxygen selectivity, defined as the fraction of oxygen atoms in the cyclic oxygenates of the total amount of oxygen in all oxygenates, a value decreasing over time from 100% to 92% is obtained. When the estimated water formation is not taken into account, all the oxygen atoms seem to end up in cyclic oxygenates reflected by an oxygen selectivity of 100%. An example of the oxygen balance and the oxygen selectivity of an epoxidation reaction as well as a detailed discussion on the cyclohexene balance is presented in the Supporting Information. Additionally, the formation of organic acids, such as butyric, valeric, caproic, hydroxyl-caproic, and adipic acid, which are all byproduct of CyOOH decomposition[4,8] was found to be negligible. This additionally confirms that indeed the epoxidation of cyclohexene with cyclohexyl hydroperoxide takes place with high selectivity.

5. CONCLUSIONS

Cyclohexyl hydroperoxide from the cyclohexane oxidation process can be employed as an oxidant for cyclohexene epoxidation. Compared to the currently commercially applied direct decomposition of CyOOH into KA-oil, this catalytic tandem route offers a way to double the yield of valuable alicyclic compounds. Ti-SiO_2 based materials were found to be highly selective in this reaction, forming only minor amounts of byproduct. The presence of accessible, isolated, tetrahedrally coordinated, Ti^{4+} sites is of vital importance for a high epoxidation activity. Moreover, our mesoporous Ti-grafted silica catalyst materials exhibit significant higher activity than the benchmark TiO_2 P25, TS-1, and Ti-BEA materials. Also the use of aqueous TBHP as oxidant yielded inferior results. From hot filtration and recycling experiments it was found that the catalyst is stable toward

dx.doi.org/10.1021/cs200354c |*ACS Catal.* 2011, 1, 1183–1192

leaching. The observed loss in activity is caused by deposition of carbonaceous species, and the catalyst could be regenerated by a calcination treatment. The cyclohexene balance thus far is not complete. From performed reference experiments it was concluded that cyclohexene disappears from the reactor probably by three causes, that is, evaporation through the septum, conversion of cyclohexene oxide, and radical degradation of cyclohexenyl hydroperoxide. From the three causes, the latter has most probably the largest effect. By tuning the hydrophobicity of the catalyst surface and the bulk olefin/peroxide ratio, an ideal ratio at the reaction site can be obtained. This increases the selectivity of the total process, by directing the mechanism from the deperoxidation to the epoxidation reaction. A combined selectivity based on peroxide conversion, toward cyclohexanol, cyclohexanone, and epoxy-cyclohexane of 170% was obtained.

■ ASSOCIATED CONTENT

Supporting Information. Additional catalytic data and a discussion on the cyclohexene balance. This material is available free of charge via the Internet at http://pubs.acs.org.

■ AUTHOR INFORMATION

Corresponding Author

*E-mail: b.m.weckhuysen@uu.nl. Phone: +31 (0)30-253 4328. Fax: +31 (0)30-251 1027.

Funding Sources

Financial support from ACTS/ASPECT is kindly acknowledged.

■ ACKNOWLEDGMENT

Tamara Eggenhuisen (Utrecht University) is thanked for the TGA and N_2-physisorption measurements and for providing the MCM-41 material. Matthijs Ruitenbeek (Dow Chemicals, Terneuzen, The Netherlands) is thanked for providing the TS-1 and Ti-BEA samples.

■ REFERENCES

(1) Schuchardt, U.; Cardoso, D.; Sercheli, R.; Pereira, R.; de Cruz, R. S.; Guerreiro, M. C.; Mandelli, D.; Spinace, E. V.; Fires, E. L. *Appl. Catal., A* **2001**, *211*, 1–17.

(2) Musser, M. T. Cyclohexanol and Cyclohexanone. In *Ullmann's Encyclopedia of Industrial Chemistry*; Wiley-VCH: Weinheim, Germany, 2005.

(3) Tolman, C. A.; Druliner, J. D.; Nappa, M. J.; Herron, N. In *Activation and Functionalization of Alkanes*, 1st ed.; Hill, C. L., Ed.; Wiley-Interscience: New York, 1989; pp 316−325.

(4) Hermans, I.; Jacobs, P.; Peeters, J. *Chem.—Eur. J.* **2007**, *13*, 754–761.

(5) Sheldon, R. A.; Kochi, J. K. *Metal-Catalyzed Oxidations of Organic Compounds*; Academic Press: New York, 1981.

(6) Kragten, U. F.; Baur, H. A. C.; Housmans, J. G. H. M., U.S. Patent 005905173, 1996, DSM N.V.

(7) Schuchardt, U.; Alves Carvalho, W.; Spinace, E. V. *Synlett* **1993**, *10*, 713–718.

(8) Hereijgers, B. P. C.; Weckhuysen, B. M. *J. Catal.* **2010**, *270*, 16–25.

(9) Anand, R.; Hamdy, M. S.; Hanefeld, U.; Maschmeyer, T. *Catal. Lett.* **2004**, *95*, 113–117.

(10) Hamdy, M. S.; Ramanathan, A.; Maschmeyer, T.; Hanefeld, U.; Jansen, J. C. *Chem.—Eur. J.* **2006**, *12*, 1782–1789.

(11) Abu-Abdoum, I. I. *Polym. Sci. B* **2008**, *50*, 9–10.

(12) Reddy, A. S.; Chen, C. Y.; Chen, C. C.; Chien, S. H.; Lin, C. J.; Lin, K. H.; Chen, C. L.; Chang, S. C. *J. Mol. Catal. A: Chem.* **2010**, *318*, 60–67.

(13) Woragamon, K.; Jongpatiwut, S.; Sreethawong, T. *Catal. Lett.* **2010**, *136*, 249–259.

(14) Mizuno, N.; Yamaguchi, K.; Kamata, K. *Coord. Chem. Rev.* **2005**, *249*, 1944–1956.

(15) Accrombessi, G. C.; Geneste, P.; Olivé, J.-L. *J. Org. Chem.* **1980**, *45*, 4139–4143.

(16) Eisenmann, J. L. *J. Org. Chem.* **1962**, *27*, 2706.

(17) Holderich, W. F.; Barsnick, U. In *Fine Chemicals through Heterogeneous Catalysis*; Sheldon, R. A., Van Bekkum, H., Eds.; Wiley-VCH: Weinheim, Germany, 2001; pp 217−231.

(18) Fasi, A.; Palinko, I. *J. Catal.* **1999**, *181*, 28–36.

(19) Shan, Z.; Yeh, C. Y.; Angevine, P. J.; Dautzenberg, F. M.; Jansen, J. C. World Patent 090324, 2005, ABB Lummus Global Inc.

(20) Zhao, D. Y.; Huo, Q. S.; Feng, J. L.; Chmelka, B. F.; Stucky, G. D. *J. Am. Chem. Soc.* **1998**, *120*, 6024–6036.

(21) Cheng, C. F.; Park, D. H.; Klinowski, J. *J. Chem. Soc., Faraday Trans.* **1997**, *93*, 193–197.

(22) Gao, X. T.; Bare, S. R.; Fierro, J. L. G.; Banares, M. A.; Wachs, I. E. *J. Phys. Chem. B* **1998**, *102*, 5653–5666.

(23) Sacaliuc, E.; Beale, A. M.; Weckhuysen, B. M.; Nijhuis, T. A. *J. Catal.* **2007**, *248*, 235–248.

(24) Bravo-Suarez, J. J.; Bando, K. K.; Lu, J.; Haruta, M.; Fujitani, T.; Oyama, S. T. *J. Phys. Chem. C* **2008**, *112*, 1115–1123.

(25) Nijhuis, T. A.; Huizinga, B. J.; Makkee, M.; Moulijn, J. A. *Ind. Eng. Chem. Res.* **1999**, *38*, 884–891.

(26) Notari, B. *Adv. Catal.* **1996**, *41*, 253–334.

(27) Berube, F.; Khadhraoui, A.; Janicke, M. T.; Kleitz, F.; Kaliaguine, S. *Ind. Eng. Chem. Res.* **2010**, *49*, 6977–6985.

(28) Berube, F.; Nohair, B.; Kleitz, F.; Kaliaguine, S. *Chem. Mater.* **2010**, *22*, 1988–2000.

(29) Morey, M. S.; O'Brien, S.; Schwarz, S.; Stucky, G. D. *Chem. Mater.* **2000**, *12*, 898–911.

(30) Klein, S.; Weckhuysen, B. M.; Martens, J. A.; Maier, W. F.; Jacobs, P. *J. Catal.* **1996**, *163*, 489–491.

(31) Trong, On, D.; Nguyen, S.; Hulea, V.; Dumitriu, E.; Kaliaguine, S. *Microporous Mesoporous Mater.* **2003**, *57*, 169–180.

(32) Chowdhury, B.; Bravo-Suarez, J. J.; Mimura, N.; Lu, J. Q.; Bando, K. K.; Tsubota, S.; Haruta, M. *J. Phys. Chem. B* **2006**, *110*, 22995–22999.

(33) Zhang, W. H.; Froba, M.; Wang, J. L.; Tanev, P. T.; Wong, J.; Pinnavaia, T. J. *J. Am. Chem. Soc.* **1996**, *118*, 9164–9171.

(34) Blasco, T.; Camblor, M. A.; Corma, A.; Perez-Pariente, J. *J. Am. Chem. Soc.* **1993**, *115*, 11806–11813.

(35) Ek, S.; Root, A.; Peussa, M.; Niinisto, L. *Thermochim. Acta* **2001**, *379*, 201–212.

(36) Vansant, E. F.; Van der Voort, P.; Vrancken, K. C. In *Characterization and Chemical Modification of the Silica Surface*; Elsevier: Amsterdam, The Netherlands, 1995; pp 59−89.

(37) Gommes, C. J.; Friedrich, H.; Wolters, M.; de Jongh, P. E.; de Jong, K. P. *Chem. Mater.* **2009**, *21*, 1311–1317.

(38) Shin, H. J.; Ryoo, R.; Kruk, M.; Jaroniec, M. *Chem. Commun.* **2001**, 349–350.

(39) Zhao, D. Y.; Feng, J. L.; Huo, Q. S.; Melosh, N.; Fredrickson, G. H.; Chmelka, B. F.; Stucky, G. D. *Science* **1998**, *279*, 548–552.

(40) Loncarevic, D.; Krstic, J.; Dostanic, J.; Manojlovic, D.; Cupic, Z.; Jovanovic, D. M. *Chem. Eng. J.* **2010**, *157*, 181–188.

(41) Petroff Saint-Arroman, R.; Didillon, B.; de Mallmann, A.; Basset, J. M.; Lefebvre, F. *Appl. Catal., A* **2008**, *337*, 78–85.

(42) Magalhaes, F. D.; Laurence, R. L.; Conner, W. C. *J. Phys. Chem. B* **1998**, *102*, 2317–2324.

(43) Bravo-Suarez, J. J.; Bando, K. K.; Fujitani, T.; Oyama, S. T. *J. Catal.* **2008**, *257*, 32–42.

(44) Lempers, H. E. B.; Sheldon, R. A. *J. Catal.* **1998**, *175*, 62–69.

(45) Franz, G.; Sheldon, R. A. *Oxidation*, 4th ed.; Wiley-VCH: Weinheim, Germany, 1972.

(46) Turra, N.; Neuenschwander, U.; Baiker, A.; Peeters, J.; Hermans, I. *Chem.—Eur. J.* **2010**, *16*, 13226–13235.
(47) Hermans, I.; Nguyen, T. L.; Jacobs, P. A.; Peeters, J. *ChemPhysChem* **2005**, *6*, 637–645.
(48) Sun, Z. Q.; Xu, J.; Du, Z. T.; Zhang, W. *Appl. Catal., A* **2007**, *323*, 119–125.
(49) Figueras, F.; Kochkar, H. *Catal. Lett.* **1999**, *59*, 79–81.